Journal of Applied Mathematics and Mechanics 72 (2008) 536–549

Contents lists available at ScienceDirect

Journal of Applied Mathematics and Mechanics

journal homepage: www.elsevier.com/locate/jappmathmech

The mixing of a viscous fluid in a layer between rotating eccentric cylinders☆

A.G. Petrov

Moscow, Russia

ARTICLE INFO

Article history:
Received 23 March 2006

ABSTRACT

The motion of an incompressible viscous fluid in a thin layer between two circular cylinders, inserted into one another, with parallel axes is investigated. The cylinders rotate relative to one another about an axis parallel to the axes of the cylinders. The stream function of the unsteady plane-parallel flow that occurs is found by solving the boundary-value problem for the equations of hydrodynamic lubrication theory. The motion of the fluid particles is found from the solution of a non-autonomous time-periodic Hamiltonian system with a Hamiltonian equal to the stream function. The positions of fluid particles over time intervals that are a multiple of the period of rotation (Poincaré points) are calculated. The set of points is investigated using a Poincaré mapping on the phase flow. The observed transition to chaotic motion is related to the mixing of the fluid particles and is investigated both numerically and using a mapping, calculated with an accuracy up to the third power of the small eccentricity. The optimum mode of motion is observed when the area of the mixing (chaos) region reaches its highest value.

The viscous fluid flow in a gap between two eccentrically situated circular cylinders, rotating around their fixed axes, was first considered by Zhukovskii in 1887. For low Reynolds numbers he obtained a biharmonic equation for the stream function and found an exact solution for it (Ref. 1, pp.121–132). In 1904 Sommerfeld [2] (see also Ref. 3, pp. 534–542) gave a simplified solution of the problem of the viscous fluid flow in the thin-layer approximation.

In 1906 Zhukovskii and Chaplygin presented an exact solution in bipolar coordinates and compared it with Sommerfeld's solution (Ref. 1, pp.133–151). Much later Ballal and Rivlin,[4] without any citations, derived Zhukovskii's and Chaplygin's accurate expression for the stream function. Sommerfeld is usually cited in the foreign literature for this work without mentioning the pioneering research of Zhukovskii and Chaplygin. The proof of the Reynolds approximation and also references to the literature on hydrodynamic lubrication theory can be found in the monographs (Refs 3,5).

In the case of a uniform rotation of the cylinders, in all the cases considered the flow region does not change with time and the flow is steady, i.e., the trajectories of the fluid particles coincide with the streamlines. In these cases the system of equations of motion of the fluid particles are integrable. There is no dynamic chaos in such systems.

Under the Zhukovskii and Chaplygin conditions of the problem, dynamic chaos can arise if the angular velocity of rotation of the cylinders depend on the time t. A slow periodic change in the angular velocities of the form $\omega(t)=\omega_0+\omega_1\cos(\varepsilon\omega t),\varepsilon\ll 1$ was considered in Ref. 6. Poincaré points over a modulation period of $2\pi/(\varepsilon\omega)$ were investigated in the adiabatic approximation. In this approximation one can use the well-known Zhukovskii–Chaplygin solution. However, the characteristic chaotization time is very long – much longer than $2\pi/(\varepsilon\omega)$.

Below we consider the extremely unsteady problem in which the frequency of variation of the flow region is identical with the frequency of rotation of the cylinders. The stream function (the Hamiltonian) has a time period equal to the period of rotation of the inner cyclinder $2\pi/\omega$, i.e., it is ε times less than the period of the Hamiltonian in the approximation considered earlier.[6] Correspondingly, the time taken for chaos to occur will also be ε times less. The stream function for this case was obtained in Refs 7,8. This solution is of interest in hydrodynamic lubrication theory, since the motion in bearings is often accompanied by wobbles, i.e., a periodic change in the centre of rotation of the inner cylinder.

☆ *Prikl. Mat. Mekh.* Vol. 72, No. 5, pp. 741-758, 2008.

E-mail address: petrov@ipmnet.ru.

0021-8928/$ – see front matter © 2008 Elsevier Ltd. All rights reserved.
doi:10.1016/j.jappmathmech.2008.11.009

1. Unsteady flow of a viscous fluid in a layer between non-coaxial rotating cylinders

A thin layer between two circular cylinders, inserted into one another, with parallel axes is filled with an incompressible viscous fluid, which is set in motion by the rotating inner cylinder with respect to the fixed outer cylinder.

In Fig. 1 we show the transverse section of the system of two cylinders, which represents the region between the two circles. The outer cylinder is fixed. Its cross section is a circle of radius R_2 with fixed centre O_2. The cross section of the inner cylinder is a circle of radius R_1 with moving centre O_1. The inner cylinder rotates with angular velocity 2ω about the axis passing through the second fixed point O, so that the point O_1 describes a circle of radius e/2 with centre O. The angle O_1 O O_2 varies with time as $\angle O_1OO_2 = 2\omega t$. It follows from the right triangle O_2O_1P that the distance between the centres O_1 and O_2 varies sinusoidally

$$O_1O_2 = e\sin\omega t \tag{1.1}$$

(see the upper right part of Fig. 1). The centre line (the x axis) is perpendicular to the cathetus O_1P and rotates with angular velocity ω.

It is more convenient to introduce another system of coordinates, in which the centre line (the x axis) is fixed (see the upper left part of Fig. 1). In this case the inner cylinder rotates with angular velocity ω, while its centre is on the x axis and oscillates sinusoidally as given by (1.1). The outer cylinder rotates in the opposite direction with velocity $-\omega$.

We will refer the radii of the cylinders to the difference $R_2 - R_1$. Then the dimensionless radii of the inner and outer cylinders will be equal to R and R + 1 respectively. By the cosine theorem, for the side O_1A of the triangle O_1O_2A we obtain the following equation for AB

$$\varepsilon^2\sin^2\omega t + (R + 1 - AB)^2 - 2\varepsilon\sin\omega t(R + 1 - AB)\cos\varphi = R^2$$

whence, when $R \gg 1$, we obtain

$$AB = 1 - \varepsilon\sin\omega t\cos\varphi + O(1/R), \quad \varepsilon = e/(R_2 - R_1) \tag{1.2}$$

where $1/R = (R_2 - R_1)/R_1$ is the relative thickness of the gap, assumed to be a small quantity, and ε is the dimensionless eccentricity, $0 \le \varepsilon < 1$.

The Reynolds criterion. The Reynolds number for the viscous fluid flow in the layer between the cylinders[3,5]

$$\mathrm{Re} = \rho\omega R_1(R_2 - R_1)/\mu \tag{1.3}$$

can be expressed in terms of the relative thickness of the gap 1/R

$$\mathrm{Re} = \rho\omega R_1^2/(\mu R)$$

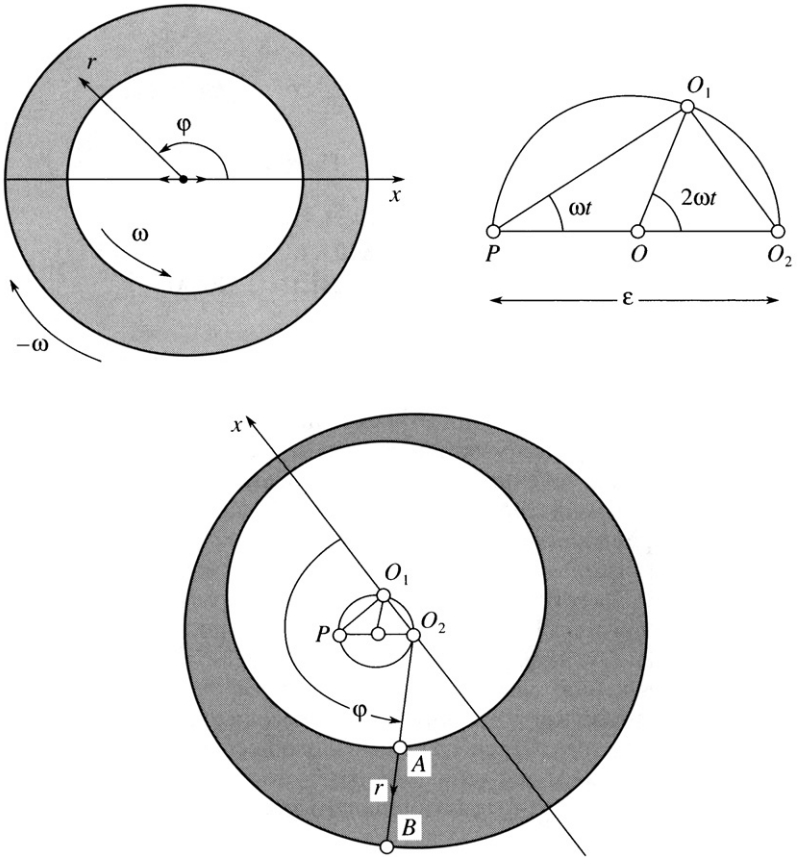

Fig. 1.

whence it can be seen that the Stokes approximation $\mathrm{Re} \ll 1$ is applicable at fairly high rotation speeds, if the relative thickness of the gap is small.

It can also be noted that, when the coaxial cylinders rotate, the Navier–Stokes equations are linear for any values of Re. Hence, the Stokes approximation will also hold when Re > 1, but for a fairly small eccentricity ε. In this connection it is useful to introduce another effective Reynolds criterion (Ref. 8, p.123) $Re_* = \rho\omega\varepsilon R_1^2/(\mu R^2)$, which is R times less than Re. Hence it follows that, for a small relative gap, the range of applicability of the Stokes approximation $\mathrm{Re}_* \ll 1$ is much wider than the region defined by Re. However, it should be noted that for fairly high Re (for coaxial rotation of the inner cylinder $Re = 41.3\sqrt{R_1/(R_2 - R_1)}$), plane-parallel flow becomes unstable.[9]

For a small relative gap $1/R \ll 1$ the linear Stokes equations can be simplified further. This simplified form of the equations was obtained by Reynolds and Sommerfeld and is the basis of hydrodynamic lubrication theory. Below we will use the equations of this approximation when

$$1/R \ll 1, \quad \mathrm{Re}_* \ll 1 \tag{1.4}$$

and the number $Re_* = \rho\omega\varepsilon R_1^2/(\mu R)$ does not exceed the critical value for which plane-parallel flow ceases to be stable.

The stream function. We will now consider the solution of the problem of the flow of a viscous incompressible fluid in a layer between two cylinders. We will use the asymptotic approximation $R \gg 1$ of hydrodynamic lubrication theory (Ref. 3, pp.534-542 and Ref. 5, pp.413-417).

We will introduce polar coordinates with centre at the point O_2: r, φ and the coordinates of the layer Y, φ (Y = R + 1 − r∈(0,Y_{max}),φ∈(0,2π)). The exact upper xlimit of the flow region Y_{max} = AB is defined by the right-hand side of Eq. (1.2)

$$Y_{\max}(t, \varphi) = 1 - \varepsilon \sin\omega t \cos\varphi \tag{1.5}$$

The components v_r,v_φ of the velocity obey the continuity equation

$$\frac{\partial v_r}{\partial r} + \frac{v_r}{r} + \frac{\partial v_\varphi}{r\partial\varphi} = 0$$

In Y, φ coordinates when $R \to \infty$ it is simplified. Neglecting small terms of the order of 1/R, we obtain for the components of the velocity $v_Y = v_r$ and v_φ

$$\frac{\partial v_Y}{\partial Y} + \frac{\partial v_\varphi}{R\partial\varphi} = 0$$

and we introduce the stream function H(t,φ,Y)

$$\frac{v_\varphi}{R} = \frac{\partial H}{\partial Y}, \quad v_Y = -\frac{\partial H}{\partial\varphi} \tag{1.6}$$

For a known stream function the coordinates of the moving fluid particles φ(t) nd Y(t) will be calculated from the system of ordinary differential equations in the Hamilton form

$$\dot\varphi = \frac{\partial H}{\partial Y}, \quad \dot Y = -\frac{\partial H}{\partial\varphi}; \quad \varphi(0) = \varphi_0, \quad Y(0) = Y_0 \tag{1.7}$$

in which the Hamiltonian is the stream function. To determine it we will write the equations of the fluid motion for $R \gg 1$

$$\frac{\partial p}{\partial Y} = 0, \quad \frac{\partial p}{R\partial\varphi} = \mu\frac{\partial^2 v_\varphi}{\partial Y^2}$$

Hence it follows that the pressure p is independent of Y. Replacing the component of the velocity v_φ by its expression in terms of the stream function, we obtain the equation

$$\frac{\partial p(t, \varphi)}{\partial\varphi} = \mu R^2\frac{\partial^3 H}{\partial Y^3} \tag{1.8}$$

According to Eq. (1.8) the function H is a cubic polynomial in Y with a coefficient of the leading power of $(\partial p/\varphi)/(6\mu R^2)$, while the remaining coefficients are found from the no-slip conditions on the surfaces of the cylinders.

Expressing the velocity components in terms of the stream function from formulae (1.6), we can write the no-slip conditions in the form

$$Y = 0\colon H = 0, \quad \frac{\partial H}{\partial Y} = -\omega \tag{1.9}$$

$$Y = Y_{\max}\colon -\frac{\partial H}{\partial\varphi} = \frac{\partial Y_{\max}}{\partial t} + \omega\frac{\partial Y_{\max}}{\partial\varphi}, \quad \frac{\partial H}{\partial Y} = \omega \tag{1.10}$$

Moreover, it is necessary to require that the condition for the pressure function p(0) = p(2π) to be

unique is satisfied, which, by virtue of Eq. (1.8), can be written in the form

$$\int_0^{2\pi} \frac{\partial^3 H}{\partial Y^3} d\varphi = 0 \tag{1.11}$$

It can be shown by direct checking that, by a suitable choice of the function Q(t,φ) the function

$$H = Q(t,\varphi)(3\tilde{Y}^2 - 2\tilde{Y}^3) + \omega Y_{\max}[-\tilde{Y}(1-\tilde{Y})^2 + \tilde{Y}^2(-1+\tilde{Y})],$$
$$\tilde{Y} = Y/Y_{\max} \tag{1.12}$$

satisfies Eq. (1.8) and all the boundary conditions (1.9)–(1.11).

To check this we write the derivative

$$\frac{\partial H}{\partial Y} = (1-\tilde{Y})\left[\frac{6Q(t,\varphi)}{Y_{\max}}\tilde{Y} + \omega(\tilde{Y}-1)\right] + \omega\tilde{Y}^2$$

Hence, when Y = 0 we have H = 0, $\partial H/\partial Y = -\omega$, i.e., boundary conditions (1.9) are satisfied.

When $Y = Y_{\max}$ we have $\tilde{Y} = 1$, $\partial H/\partial Y = \omega$, i.e., the first condition of (1.10) is satisfied. Further, when $Y = Y_{\max}$ we obtain $\partial H/\partial\tilde{Y} = Y_{\max}\omega$ and

$$H = Q(t,\varphi), \quad \frac{\partial H}{\partial\varphi} = \frac{\partial Q(t,\varphi)}{\partial\varphi} + \frac{\partial H}{\partial\tilde{Y}}\frac{\partial\tilde{Y}}{\partial\varphi} = \frac{\partial Q(t,\varphi)}{\partial\varphi} - \omega\frac{\partial Y_{\max}}{\partial\varphi}$$

Substituting the expression for $\partial H/\partial\varphi$ into the second boundary condition of (1.10), we obtain the equation of conservation of mass in the layer

$$\frac{\partial Q}{\partial\varphi} + \frac{\partial Y_{\max}}{\partial t} = 0$$

Hence it follows that Q(t,φ) is the fluid flow rate through the section, of the layer with coordinate φ. Integrating this equation up to the additive function of time, we obtain Q

$$Q = \varepsilon\omega\cos\omega t\sin\varphi \tag{1.13}$$

This function of time is found from the condition for the pressure (1.11) to be unique and is equal to zero.

Substituting the third derivative of the Hamiltonian into Eq. (1.8), we obtain the pressure

$$p(\varphi) = 6\omega\mu R^2\left[\frac{\cos\omega t}{Y_{\max}^2\sin\omega t} + c(t)\right]$$

The function c(t), which is independent of the coordinates in hydrodynamic lubrication theory, usually remains an undetermined quantity,[3,5] and the forces and moments acting on the cylinder do not depend on its value. In this problem it is more convenient to take it to be equal to -ctgωt.

We then obtain for the pressure

$$p(\varphi) = 6\varepsilon\omega\mu R^2\cos\omega t\cos\varphi\frac{2-\varepsilon\sin\omega t\cos\varphi}{(1-\varepsilon\sin\omega t\cos\varphi)^2} \tag{1.14}$$

Substituting expression (1.13) into (1.12), we obtain the Hamiltonian

$$H(t,\varphi,Y) = \omega\varepsilon\cos\omega t\sin\varphi(3\tilde{Y}^2 - 2\tilde{Y}^3) + \omega(\tilde{Y}-\tilde{Y}^2)Y_{\max} \tag{1.15}$$

The velocity field is expressed in terms of it using formulae (1.6), knowing which and the pressure field (1.14), we can calculate the forces and moments acting on the cylinder. This is usually also the main aim of the investigation. In this paper we are interested in the problem of investigating the nature of the motion of the fluid particles in the velocity field obtained.

2. The motion of particles of a viscous fluid in a layer between the cylinders

Poincaré points. Numerical calculation. The locations of the points φ_n, Y_n at instants of time $t_n = 2\pi n/\omega$ are found from the solution of the Cauchy problem for the Hamilton Eq. (1.7).

These points are called Poincaré points (PPs).

At instants of time t_n the axes O_1 and O_2 of the inner and outer cylinders coincide, and the flow region, in φ, Y variables, is a rectangle $\varphi\in(0,2\pi)$, $Y\in(0,1)$. In Fig. 2 we show the PP in the φ, Y plane for different values of the parameter ε, obtained by numerical solution of Eq. (1.7) using the Runge–Kutta method. The points are derived at instants of time $t_n = 2\pi n/\omega$ ($n = 0, 1, \cdots, 500$), for which the axes of the cylinders O_1 and O_2 coincide. The initial points are denoted by crosses. When $\varepsilon = 0$ the Hamiltonian $H = \omega(y - y^2)$ defines an integrable Hamilton system, corresponding to simple Couette flow. The points lie on integral curves Y = const (in polar coordinates these are concentric circles). For a small value of the parameter $\varepsilon = 0.1$ the pattern is close to an unperturbed one. Each series of PP, starting from a single initial point, lies on its own invariant curve. For this case the system can be approximated fairly accurately by an integrable Hamilton system by the

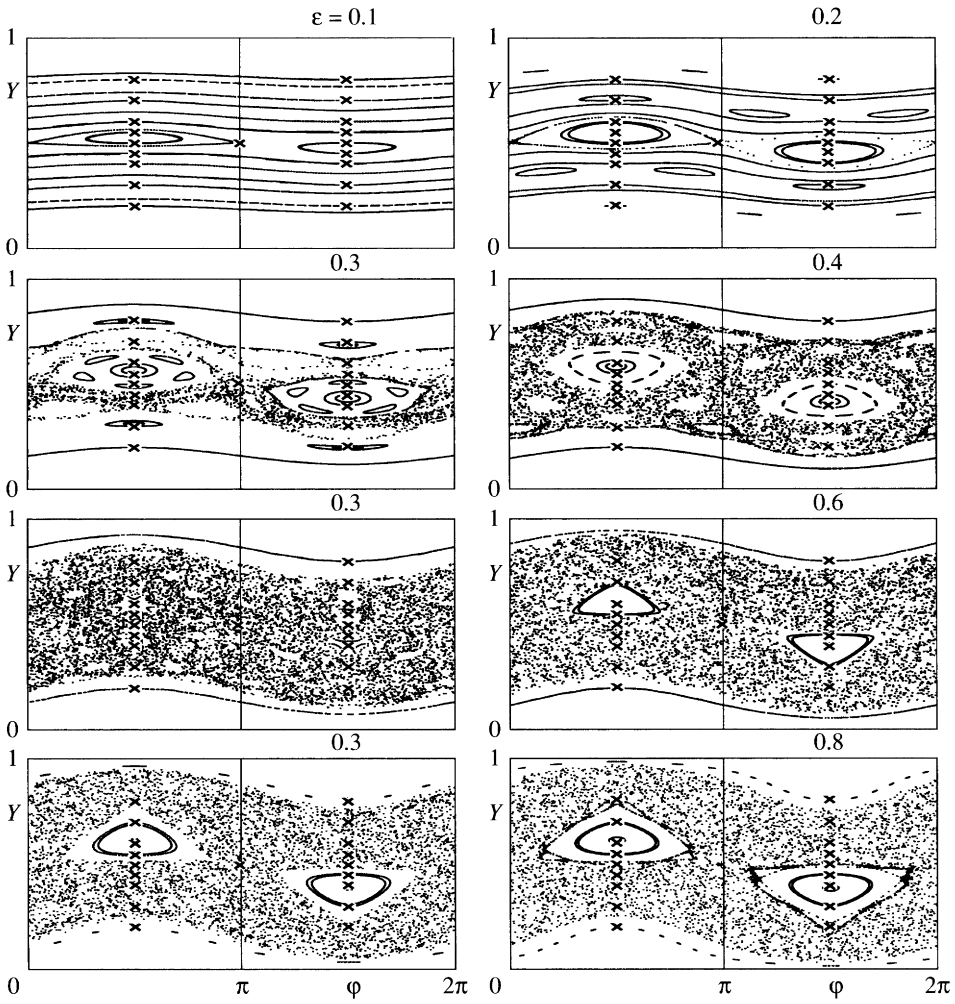

Fig. 2.

standard averaging method. For a value of $\varepsilon = 0.2$ the phase pattern is already complicated. Some series of PPs, starting from a single initial point, lie on several unconnected invariant curves rather than only one. When $\varepsilon = 0.3$ the number of such curves is very large. Some series occupy areas rather than curves. Such behaviour of the PPs [10–13] is typical for dynamic chaos. The transition to chaos is generated in the neighbourhood of the point $\varphi = \pi$, $Y = 1/2$. It can be seen from Fig. 2 that the greatest area of chaos is reached when $\varepsilon \approx 0.5$. When $\varepsilon > 0.5$ two subregions with invariant PPs curves grow as ε increases in the middle of the flow region. The PP of these never fall in these subregions. Hence, the greatest mixing occurs when $\varepsilon \approx 0.5$.

Approaches to investigating dynamic chaos and mixing in hydrodynamic systems. In the theory of dynamical systems, the idea of dynamic chaos is related to the presence of a positive Lyapunov exponent of a discrete trajectories on an attractor in the case of Lyapunov instability, or with the non-integer Hausdorff dimension of the attractor. Rigorous and complete justification using these definitions for the given and fairly complex Hamilton system is hardly possible. Hence, only an intuitive approach is used at the present time in papers on hydrodynamics. For example, in Ref. 6, although the results of mathematical investigations are also cited, they are not used for strict proofs, and the regions of dynamic chaos were established on the patterns for Poincaré points obtained numerically.

Here we will follow a non-rigorous but intuitively understandable and clear definitions of dynamic chaos, starting from the phase patterns. We will cite the definitions [14] for a qualitative description of the effects related to the phenomena of dynamic chaos and mixing, reflected in Fig. 2. The trajectory of a Lagrange particle of fluid is found from the solution of problem (1.7), while a PP is the track of a particle obtained using a cinecamera with a frame frequency corresponding to the period T. The PPs form a denumerable set of points in a plane, which depends, generally speaking, on t_0, X_0 and Y_0. If the set of PPs belongs to a one-dimensional line, this line is called an invariant curve. For ordered motion, all sets of PPs form a family of invariant curves, which continuously fill the flow region (the case of ordered motion of the particles is given below for $\varepsilon = 0.1$ and $\varepsilon = 0.2$). In the other case, the set of PPs fills a two-dimensional region. This case ($\varepsilon > 0.2$) will also be called chaotic motion of PPs.

For steady fluid motion, the invariant curves lie on the streamlines, which continuously fill the flow region, and there will be no chaos. A chaotic situation can only arise in extremely unsteady flows. When the Hamiltonian depends periodically on the time, the set of PPs can be calculated using the recurrence formulae $X_n = P^T_{t_o}(X_{n-1})$, where $P^{\Delta t}_{t0}$, $(\Delta t = t - t_0)$ is the mapping on the phase flow of system (1.7), or simply the solution of problem (1.7). The mapping in the period P^T_{t0} is called a Poincaré mapping.

The definition of a chaotic situation introduced above does not depend on t_0.[14] To be specific we will choose $t_0 = 0$, and we will dispense with the superscripts and subscripts in the notation of the Poincaré mapping: $P^T_0 = P$.

The investigation of the chaotic nature of the motion using Poincaré mappings will also be called the method of Poincaré sections. References 10, 12 and 13 are devoted to this theme, but the definition of Poincaré mapping itself is a complex computational problem. Hence, the Poincaré points will usually be found numerically, but analytical methods will only be used for very simple systems.

An analytical method of constructing a Poincaré mapping. In Fig. 2 the occurrence of chaos is also demonstrated in direct numerical solutions of Hamilton's equations. It is of interest to obtain, in analytical form, those Poincaré mappings which might describe the transition to dynamic chaos as ε increases, as close as possible to those shown in Fig. 2. For this purpose we will use a method of constructing the mapping in parametric form.[14] The analytical mapping obtained in this way gave phase portraits of the PPs which are practically identical with the numerical ones, and describes chaotic situations. The analytical form of the mapping enables us to apply methods to it that are well known from the theory of dynamical systems, in particular, the method of Lyapunov exponents for investigating the stability of fixed points.

We will present, in a brief form, formulae [14] for constructing a Poincaré mapping of a system with Hamiltonian H(t,q,p).

The mapping $(X_0,Y_0)\to(X_1,Y_1)$ in a period T will be calculated parametrically

$$X_0 = x-\frac{1}{2}\Psi_y,\quad Y_0 = y+\frac{1}{2}\Psi_x,$$
$$X_1 = x+\frac{1}{2}\Psi_y,\quad Y_1 = y-\frac{1}{2}\Psi_x \tag{2.1}$$

The function $\Psi(x,y)$ is expressed in terms of the function $\psi(t,x,y)$, which is found from the solution of the Cauchy problem for a Hamilton–Jacobi type equation

$$\psi_t(t,x,y) = H\left(t, x+\frac{1}{2}\psi_y(t,x,y), y-\frac{1}{2}\psi_x(t,x,y)\right),\quad \psi(0,x,y) = 0. \tag{2.2}$$

Its value at the instant of time t = T defines the parametric mapping function (2.1): $\psi(x,y)=\psi(T,x,y)$. For the Hamiltonian of the standard system

$$H = \varepsilon H_1+\varepsilon^2 H_2+\varepsilon^3 H_3+\ldots \tag{2.3}$$

with a small parameter ε, the function $\Psi(x,y)$ is calculated in the form of a series in powers of the small parameter ε

$$\Psi = \int_0^T\left[\varepsilon H_1(t,x,y)+\varepsilon^2\left(H_2(t,x,y)-\frac{1}{2}\left\{H_1,\int_0^t H_1\,dt'\right\}\right)\right]dt+\ldots$$
$$(\{f,h\} = f_y h_x - f_x h_y) \tag{2.4}$$

The mapping (2.1) possesses an important property: when the following condition is satisfied

$$J = 1+\frac{1}{4}(\Psi_{xx}\Psi_{yy}-\Psi_{xy}^2)>0$$

it exactly conserves the phase volume. Consequently, for an arbitrary function $\Psi(x,y)$, $J>0$, the points (X_n,Y_n),$(n=0,1,2\cdots)$ calculated by this mapping will be PPs of a certain Hamilton system. If the function $\Psi(x,y)$ is close to the exact solution of problem (2.2), then the phase pattern of the PPs calculated using mapping (2.1) will also be close to the pattern of PPs of the initial Hamilton system.

We will show how to construct an analytical expression for the function $\Psi(x,y)$ with an error of the order of ε^3. The initial Hamiltonian (1.15) for the expansion in powers of ε has a term $H_0(Y)$, which depends only on Y. In this case the Hamiltonian can be reduced to standard form by a canonical replacement of variables $(X,Y)\to(\bar{X},\bar{Y})$ using the generating function

$$S(t,\tilde{X},Y) = -tH_0(Y)-\tilde{X}Y$$

The variables and the Hamiltonian are converted as follows:

$$X = -\frac{\partial S}{\partial Y} = \tilde{X}+t\frac{dH_0}{dY},\quad \tilde{Y} = -\frac{\partial S}{\partial\tilde{X}} = Y$$
$$\tilde{H} = \frac{\partial S}{\partial t}+H = \varepsilon H_1\left(t,\tilde{X}+t\frac{dH_0}{dY},\tilde{Y}\right)+\ldots \tag{2.5}$$

and expansion (2.4) is then used. In the new Hamiltonian the term, independent of ε, is eliminated, and the expansion begins from a small term of the order of magnitude of ε. This expansion is called a standard form.

3. The Poincaré mapping. Reduction of the Hamiltonian to standard form

To reduce the Hamiltonian (1.15) to standard form we make two canonical replacements. We will use the apparatus of generating functions.

The first replacement $\varphi, Y \to \tilde{q}, \tilde{p}$ maps the region of the flow with curvilinear boundaries $\varphi\in(0,2\pi Y\in(0,Y_{\max}))$ into a rectangle $q\in(0, 2\pi)$, $\tilde{p}\in(-1/2, 1/2)$. It has the generating function

$$S_1(\varphi, \tilde{p}) = \left(\frac{1}{2} + \tilde{p}\right)\int_0^{\varphi} Y_{\max} d\varphi = \left(\frac{1}{2} + \tilde{p}\right)(\varphi - \varepsilon \sin\omega t \sin\varphi)$$

From well-known formulae we determine the analytical form of the replacement

$$\tilde{q} = \frac{\partial S_1}{\partial \tilde{p}} = \varphi - \varepsilon \sin\omega t \sin\varphi, \quad Y = \frac{\partial S_1}{\partial \varphi} = \left(\frac{1}{2} + \tilde{p}\right)Y_{\max} \tag{3.1}$$

and the Hamiltonian in the new variables

$$\tilde{H}(t, \tilde{q}, \tilde{p}) = \frac{\partial S_1}{\partial t} + H = -\omega\tilde{p}^2 + \varepsilon\omega\left(\tilde{p}^2 - \frac{1}{4}\right)[\sin\omega t\cos\varphi - 2\tilde{p}\cos\omega t\sin\varphi]$$

The relation $\varphi(t, \tilde{q})$ is defined by the first Equation of (3.1).

The second canonical replacement cancels out the first term, which is independent of ε, in the Hamiltonian, and reduces the system to the standard form $\tilde{q}, \tilde{p} \to q, p$. The generating function of the replacement is constructed using formula (2.5)

$$S_2(t, q, \tilde{p}) = \omega t\tilde{p}^2 - q\tilde{p}$$

We find the analytical form of the replacement and the converted Hamiltonian in terms of it

$$\tilde{q} = -\frac{\partial S_2}{\partial \tilde{p}} = q - 2p\omega t \quad p = -\frac{\partial S_2}{\partial q} = \tilde{p} \tag{3.2}$$

$$\tilde{\tilde{H}}(t, q, p) = \varepsilon\omega F(t, \varphi, p), \quad F = \left(p^2 - \frac{1}{4}\right)(\sin\omega t\cos\varphi - 2p\cos\omega t\sin\varphi) \tag{3.3}$$

The function $\varphi = \varphi(t,q,p,)$ is determined implicitly from the equation

$$\varphi - \varepsilon \sin\omega t \sin\varphi = q - 2p\omega t \tag{3.4}$$

The equations of motion of a particle in q, p variables have the form

$$\dot{q} = \frac{\partial \tilde{\tilde{H}}}{\partial p} = \varepsilon\omega\left(\frac{\partial F}{\partial p} - \frac{2\omega t}{Y_{\max}}\frac{\partial F}{\partial \varphi}\right), \quad \dot{p} = -\frac{\varepsilon\omega}{Y_{\max}}\frac{\partial F}{\partial \varphi} \tag{3.5}$$

From equality (3.4) we can obtain

$$\frac{\partial \varphi}{\partial t} = \frac{1}{Y_{\max}}(-2p\omega + \varepsilon\omega\cos\omega t\sin\varphi), \quad \frac{\partial \varphi}{\partial q} = \frac{1}{Y_{\max}}, \quad \frac{\partial \varphi}{\partial p} = -\frac{2\omega t}{Y_{\max}}$$

$$\dot{\varphi} = \frac{\partial \varphi}{\partial t} + \dot{q}\frac{\partial \varphi}{\partial q} + \dot{p}\frac{\partial \varphi}{\partial p} \tag{3.6}$$

Using the formulae obtained for the derivatives, we can write the equations of motion of a particle (3.5) in the initial variables φ, Y

$$\frac{d\varphi}{d\omega t} = -2p - 6\frac{\varepsilon}{Y_{\max}}\left(p^2 - \frac{1}{4}\right)\cos\omega t\sin\varphi$$

$$\frac{dp}{d\omega t} = \frac{\varepsilon}{Y_{\max}}\left(p^2 - \frac{1}{4}\right)(\sin\omega t\sin\varphi + 2p\cos\omega t\cos\varphi), \quad Y = \left(\frac{1}{2} + p\right)Y_{\max}. \tag{3.7}$$

This system of equations is equivalent to the initial system (1.7). Hence we can obtain the PPs numerically, and the result will be identical with that obtained above.

The Pointcaré mapping enables the PPs to be calculated from recurrence relations. Writing the expansion of Hamiltonian (3.3)

$$\tilde{\tilde{H}}(\tau, q, p) = \varepsilon\omega H_1 + \varepsilon^2\omega H_2 + O(\varepsilon^3),$$

$$H_1 = \left(p^2 - \frac{1}{4}\right)(\sin\tau\cos(q - 2p\tau) - 2p\cos\tau\sin(q - 2p\tau)),$$

$$H_2 = -\left(p^2 - \frac{1}{4}\right)\left[\sin^2\tau\sin^2(2(q - 2p\tau)) + \frac{1}{2}\sin 2\tau\sin(2(q - 2p\tau))\right],$$

$$\tau = \omega t \tag{3.8}$$

and using formula (2.4), we can obtain the Poincaré mapping with an accuracy of up to ε^3. Reverting to the initial variables φ, Y and using transformations (3.1) and (3.2) we obtain a mapping for the PP $(\varphi_0,Y_0)\to(\varphi_1,Y_1)$ in the form of the superposition of three mappings

$$(\varphi_0, Y_0)\to(Q_0, p_0),\quad (Q_0, p_0)\to(Q_1, p_1),\quad (Q_1, p_1)\to(\varphi_1, Y_1)$$

The first and third are mappings of the displacement

$$1)\ p_0 = Y_0-\frac{1}{2},\quad Q_0 = \varphi_0-2\pi p_0,$$

$$3)\ Y_1 = p_1+\frac{1}{2},\quad \varphi_1 = Q_1-2\pi p_1, \tag{3.9}$$

The intermediate mapping $(Q_0,p_0)\to(Q_1,p_1)$ is found in the parametric form (2.1)

$$2)\ Q_0 = x'-\frac{1}{2}\Psi_y,\quad p_0 = y+\frac{1}{2}\Psi_{x'};\quad Q_1 = x'+\frac{1}{2}\Psi_y,\quad p_1 = y-\frac{1}{2}\Psi_{x'} \tag{3.10}$$

in which the function $\Psi(x',y)$ is calculated using series (2.4)

$$\Psi(x', y) = \varepsilon\Psi_1(x', y)+\varepsilon^2\Psi_2(x', y)+O(\varepsilon^3)$$

$$\Psi_1(x', y) = -2f(y)\sin x',\quad \Psi_2(x', y) = u(y)+\upsilon(y)\cos(2x')$$

$$f(y) = \left(y^2-\frac{1}{4}\right)\sin 2\pi y$$

$$u(y) = \pi\left(y^2-\frac{1}{4}\right)^2\left(\frac{5}{2}-\cos 4\pi y\right)-yg(y)$$

$$\upsilon(y) = \pi\left(y^2-\frac{1}{4}\right)^2-\left(y^2-\frac{5}{8}\right)\frac{g(y)}{4y}$$

$$g(y) = \left(y^2-\frac{1}{4}\right)\sin 4\pi y \tag{3.11}$$

The mapping (3.9), (3.10) and (3.11) obtained can be refined considerably if we represent the mapping in a period in the form of two mappings over a half-period. The centres of the cylinders also coincide at instants of time that are multiples of a half-period. The region φ, Y at these instants of time is also a rectangle. The mappings are constructed similarly in the form of the superposition of three mappings: in the first half-period

$$(\varphi_0, Y_0)\to(Q_0, p_0)\to(Q_{1/2}, p_{1/2})\to(\varphi_{1/2}, Y_{1/2})$$

in the second half-period

$$(\varphi_{1/2}, Y_{1/2})\to(Q_{1/2}, p_{1/2})\to(Q_1, p_1)\to(\varphi_1, Y_1)$$

The analytical form of the mapping $(\varphi_0,Y_0)\to(\varphi_{1/2},Y_{1/2})$ in the first half-period has the form

$$1)\ p_0 = Y_0-\frac{1}{2},\quad Q_0 = \varphi_0-\pi p_0,$$

$$Q_0 = x'-\frac{1}{2}\Phi_y,\quad p_0 = y+\frac{1}{2}\Phi_{x'}$$

$$2)\ Q_{1/2} = x'+\frac{1}{2}\Phi_y,\quad p_{1/2} = y-\frac{1}{2}\Phi_{x'}$$

$$\varphi_{1/2} = Q_{1/2}-\pi p_{1/2},\quad Y_{1/2} = p_{1/2}+\frac{1}{2} \tag{3.12}$$

and in the second half-period the mapping $(\varphi_{1/2},Y_{1/2})\to(\varphi_1,Y_1)$ differs only by a parametric function

$$1)\ p_{1/2} = Y_{1/2}-\frac{1}{2},\quad Q_{1/2} = \varphi_{1/2}-\pi p_{1/2}$$

$$Q_{1/2} = x-\frac{1}{2}\tilde{\Phi}_y,\quad p_{1/2} = y+\frac{1}{2}\tilde{\Phi}_x$$

$$2)\ Q_x = x+\frac{1}{2}\tilde{\Phi}_y,\quad p_1 = y-\frac{1}{2}\tilde{\Phi}_x$$

$$3)\ \varphi_1 = Q_1-\pi p_1,\quad Y_1 = p_1+\frac{1}{2} \tag{3.13}$$

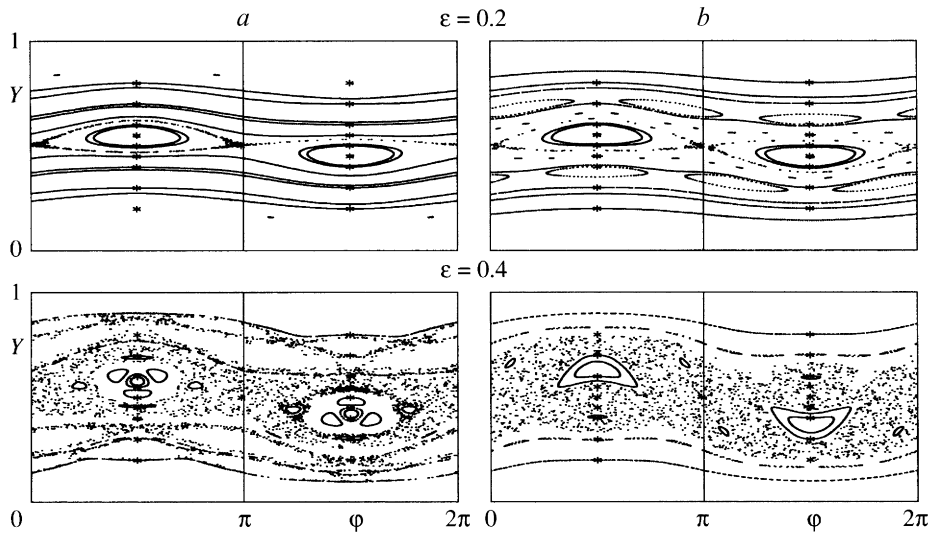

Fig. 3.

The functions Φ and $\tilde{\Phi}$ are calculated as

$$\Phi(x, y) = \varepsilon\Phi_1(x, y) + \varepsilon^2\Phi_2(x, y) + O(\varepsilon^3)$$
$$\tilde{\Phi}(x, y) = -\varepsilon\Phi_1(x, y) + \varepsilon^2\Phi_2(x, y) + O(\varepsilon^3)$$
$$\Phi_1(x, y) = 2\left(y^2 - \frac{1}{4}\right)\cos x\cos(\pi y), \quad \Phi_2(x, y) = u(y) + v(y)\cos(2x)$$
$$u(y) = \frac{5\pi}{4}\left(y^2 - \frac{1}{4}\right)^2 + \frac{\pi}{2}\left(y^2 - \frac{1}{4}\right)^2\cos 2\pi y + yf(y)$$
$$v(y) = -\frac{\pi}{2}\left(y^2 - \frac{1}{4}\right)^2 - \left(y^2 - \frac{5}{8}\right)\frac{f(y)}{4y} \tag{3.14}$$

The function f(y) is defined by the fourth equality of (3.11).

The residual term of the mappings obtained is of the order of $(T\varepsilon)^3$, where T is the time interval. Hence, a mapping over two half-periods has only a quarter of the error compared with mapping over a period. Mapping over a period is applicable provided $J > 0$, which is satisfied in the interval $0 < \varepsilon < 0.45$, while the mapping over two half-periods is applicable over a greater range: $J > 0$: $0 < \varepsilon < 0.59$.

In Fig. 3 we show phase portraits of the PPs when $\varepsilon = 0.2$ and $\varepsilon = 0.4$, obtained using the analytical Poincaré mapping: (a) over one period from the solution of the algebraic Eqs. (3.9)–(3.11) and for comparison (b) – over two half-periods from the solution of Eqs. (3.12)–(3.14). A comparison of Fig. 3 with the corresponding phase portraits in Fig. 2 shows that they not only agree qualitatively but also quantitatively. Thus, the positions of the fixed points, denoted by the small circles, practically coincide. The elliptic and hyperbolic points correspond to one another. The regions of chaos of the points and their ordered motion differ very little on corresponding parts of the figures. The phase portraits in Fig. 3*b* (over two half-periods) agree better with the exact calculations, presented in Fig. 2, than the phase portraits in Fig. 3*a* (over a single period).

The phase portrait presented in Fig. 4 for $\varepsilon = 0.5$ is defined by formulae (3.12)–(3.14), while the mapping (3.9)–(3.11) does not exist in this case.

Hence, when $\varepsilon < 0.5$ the accuracy of the functions (3.11) and (3.14) and the parametric mappings obtained with them are sufficient to determine the phase trajectories of the PPs and to describe the transition to chaos.

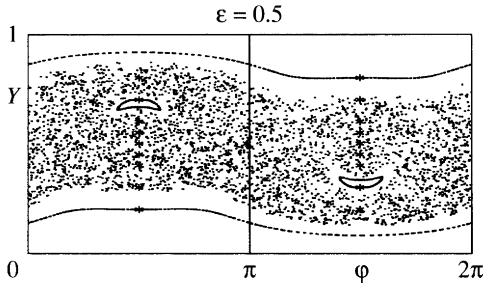

Fig. 4.

4. Fixed points of the Poincaré mapping

The phase portrait of the PPs can be described qualitatively if we obtain the fixed points of the mapping and investigate their stability. Stable fixed points are called elliptic-type points. In the neighbourhood of such a point the PPs lie on closed invariant curves, close to ellipses. The corresponding motion is ordered.

Unstable fixed points are called hyperbolic-type points. In the neighbourhood of such a point the arrangement of the PPs may be chaotic.

The main fixed points of the mapping $(\varphi_0,Y_0)\to(\varphi_1,Y_1)$ are determined from the system of equations

$$Y_0 = Y_1,\ \varphi_0 = \varphi_1$$

They can be sought in the form of an asymptotic expansion in $\varepsilon \ll 1$. From mapping (3.9)–(3.11) for the fixed points we obtain

$$p_0 = p_1 = y,\quad Y_0 = Y_1 = 1/2 + y,\quad \varphi_0 = \varphi_1 = x' \tag{4.1}$$

$$\Psi_{x'} = -2\varepsilon\cos x'(f(y) + 2\varepsilon\upsilon(y)\sin x') = 0$$

$$\Psi_y - 4\pi y = \varepsilon^2(u'(y) + \upsilon'(y)\cos 2x') - 2\varepsilon f'(y)\sin x' - 4\pi y = 0 \tag{4.2}$$

System (4.2) is equivalent to two systems of equations

$$\cos x' = 0$$

$$\varepsilon^2(u'(y) - \upsilon'(y)) - 2\varepsilon f'(y)\sin x' - 4\pi y = 0 \tag{4.3}$$

$$f(y) + 2\varepsilon\upsilon(y)\sin x' = 0$$

$$\varepsilon^2(u'(y) + \upsilon'(y)\cos 2x') - 2\varepsilon f'(y)\sin x' - 4\pi y = 0 \tag{4.4}$$

The first system (4.3) has two roots, which can be obtained using asymptotic expansions in powers of y. The points corresponding to these roots have the form $M_1(\pi/2,1/2+y)$ and $M_2(3\pi/2,1/2-y)$, and y is

obtained from the equation

$$\varepsilon = 4y + 104y^3,\quad y \in (0, 0.1) \tag{4.5}$$

System (4.4) for any ε has two solutions

$$M_3(0, 1/2),\quad M_4(\pi, 1/2) \tag{4.6}$$

and, moreover, when $\varepsilon > 0.587$ it has solutions determined by the asymptotic expansions ($\varepsilon = 0.587 + 17.7y^2 + \ldots, \sin x' = -4.54y - 32.2y^3 + \ldots$). However, when $\varepsilon > 0.5$ the mapping obtained is inapplicable, and hence the last solution will not be considered.

The fixed points obtained correspond to periodic solutions of Hamilton's equations with period $\omega t = 2\pi$. Series of fixed points also exist corresponding to the period $2\pi n$. These points are found from the equations $\phi_n = \phi_0 + 2\pi k$, $p_n = p_0$ and they can also be found analytically. We will confine ourselves to considering the stability of the fixed points (4.5) and (4.6).

The stability of the fixed points. The stability of a fixed point of the mapping $(\varphi_0,Y_0)\to(\varphi_0,Y_0)$ can be investigating using the linearised mapping in its neighbourhood

$$\begin{Vmatrix} d\varphi_1 \\ dY_1 \end{Vmatrix} = A \begin{Vmatrix} d\varphi_0 \\ dY_0 \end{Vmatrix} \tag{4.7}$$

The matrix of the mapping A can be represented in the form of the product of the matrices of the linearized mappings 1) (3.9), 2) (3.10) and 3) (3.9)

$$\begin{Vmatrix} d\varphi_1 \\ dY_1 \end{Vmatrix} = B \begin{Vmatrix} dQ_1 \\ dp_1 \end{Vmatrix},\quad \begin{Vmatrix} dQ_1 \\ dp_1 \end{Vmatrix} = \Psi_+ \begin{Vmatrix} dx \\ dy \end{Vmatrix}$$

$$\begin{Vmatrix} dx \\ dy \end{Vmatrix} = \Psi_-^{-1} \begin{Vmatrix} dQ_0 \\ dp_0 \end{Vmatrix},\quad \begin{Vmatrix} dQ_0 \\ dp_0 \end{Vmatrix} = B \begin{Vmatrix} d\varphi_0 \\ dY_0 \end{Vmatrix}$$

The matrices of the mappings have the form

$$B = \begin{Vmatrix} 1, & -2\pi \\ 0, & 1 \end{Vmatrix},\quad \Psi_\pm = \begin{Vmatrix} 1 \pm b & \pm c \\ \mp a & 1 \mp b \end{Vmatrix}$$

The quantities a, b and c are expressed in terms of the second derivatives of the parametric function $\Psi(x,y)$

$$a = \frac{1}{2}\Psi_{xx} = \varepsilon f(y)\sin x - 2\varepsilon^2 v(y)\cos 2x$$

$$b = \frac{1}{2}\Psi_{xy} = \varepsilon f'(y)\cos x - \varepsilon^2 v'(y)\sin 2x$$

$$c = \frac{1}{2}\Psi_{yy} = -\varepsilon f''(y)\sin x + \frac{1}{2}\varepsilon^2(u''(y) + v''(y)\cos 2x)$$

Hence we obtain

$$A = B\Psi_+\Psi_-^{-1}B$$

We have the following expression for the trace of the matrix A

$$I = a_{11} + a_{22} = 2\frac{1 + b^2 + 4\pi a - ca}{1 - b^2 + ca} \tag{4.8}$$

The characteristic equation of the linear mapping (4.7) $m^2 - \mathrm{Im} + 1 = 0$ when $|I| \le 2$ has complex roots, the moduli of which are equal to unity: $|m_1| = |m_2| = 1$. In this case the fixed points will be stable (elliptic-type points). Otherwise the roots are real, one of the roots is greater than unity ($m_1 > 1$), and the fixed point will be unstable (a hyperbolic-type point). Taking expression (4.8) into account, the stability condition will have the form

$$\left|\frac{I}{2}\right| = \left|\frac{1 + b^2 + 4\pi a - ca}{1 - b^2 + ca}\right| < 1 \tag{4.9}$$

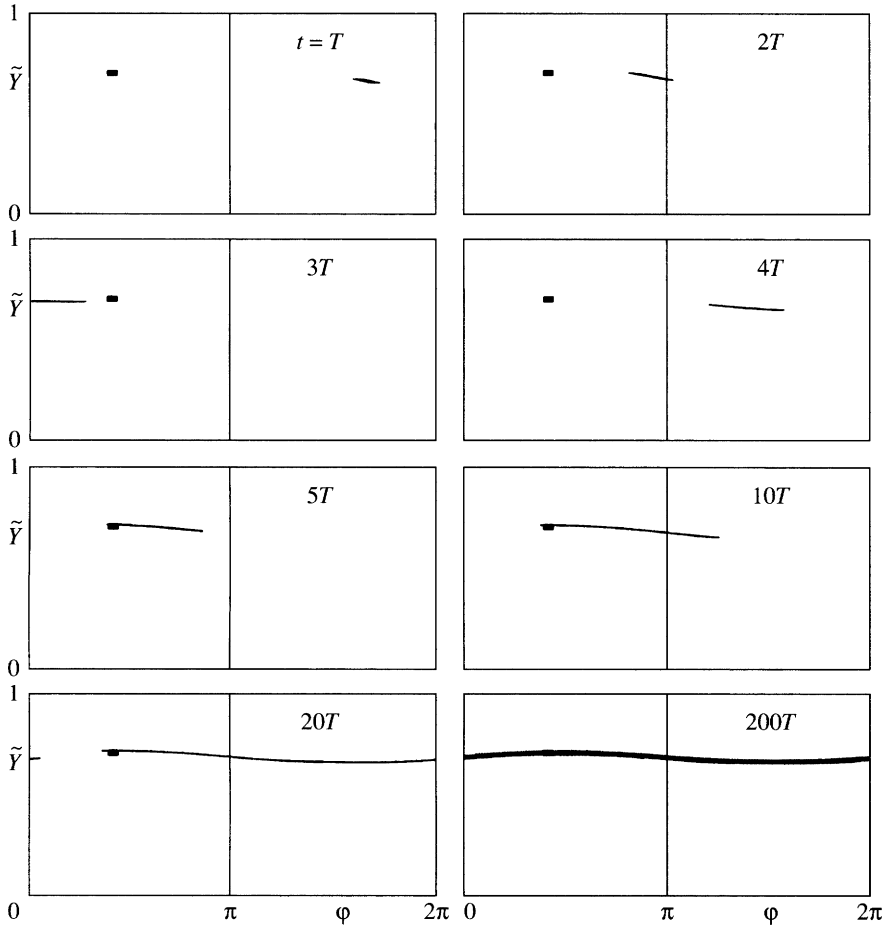

Fig. 5.

We will investigate the stability of the fixed point $M_1(\pi/2,1/2+y)$ (4.5). With an accuracy up to ε^3 we obtain

$$a = -\frac{3}{16}\varepsilon^2\pi - \frac{1}{2}\varepsilon\pi y + 2\varepsilon^2\left(\frac{3}{8}\pi + \frac{5}{12}\pi^3\right)y^2 + \ldots = \varepsilon\left(\frac{1}{3}\pi^3 + 2\pi\right)y^3 + O(y^4),$$

$$b = 0, \quad c = \frac{1}{2}\varepsilon^2\left(\frac{1}{6}\pi^3 - \frac{1}{4}\pi\right) + (-\varepsilon(2\pi^3 + 12\pi))y$$

and, according to equality (4.5), the stability condition (4.9) takes the form

$$|I/2| = \left|1 + (-20\pi^2)y^2 + O(y^3)\right| < 1$$

If we neglect terms $O(y^3)$, we can obtain an estimate of the stability region of the fixed point $M_1(\varphi = \pi/2, Y = 1/2 + \varepsilon/4 + O(\varepsilon^3))$: $0 < y < 1/(\pi\sqrt{10}) \approx 0.1$ and, taking equality (4.5) into account, $\varepsilon < 0.4$, which agrees with the estimates previously obtained.[7]

Second, the symmetrically positioned fixed point $M_2(\varphi = 3\pi/2, Y = 1/2 - \varepsilon/4 + O(\varepsilon^3))$ is stable for all values of the parameter ε. These conclusions are confirmed by a numerical experiment (Fig. 2). When $\varepsilon = 0.1$, 0.2, 0.3 and 0.4 the points M_1 and M_2 are of the elliptic type. In their neighbourhood the PPs are situated on closed invariant curves. When $\varepsilon = 0.5$ the fixed points M_1 and M_2 cease to be stable and the PPs chaotically fill almost the whole flow region.

The stability of the fixed point $M_3(0,1/2)$ (4.6) can be investigated similarly. In this case

$$a = \frac{3}{16}\pi\varepsilon^2, \quad b = -\frac{1}{2}\pi\varepsilon, \quad c = \frac{11}{12}\pi^3 + \frac{5}{8}\pi\varepsilon^2$$

Substitution into stability condition (4.9) gives

$$I/2 = 1 + (5\pi^2/4)\varepsilon^2 + O(\varepsilon^4) > 1$$

Hence it follows that the fixed point $M_3(\varphi = 0, Y = 1/2)$ is unstable at least for small values of the parameter ε, that is, it is a hyperbolic-type point. The point $M_4(\varphi = \pi, Y = 1/2)$ is unstable for the same values of ε as M_3.

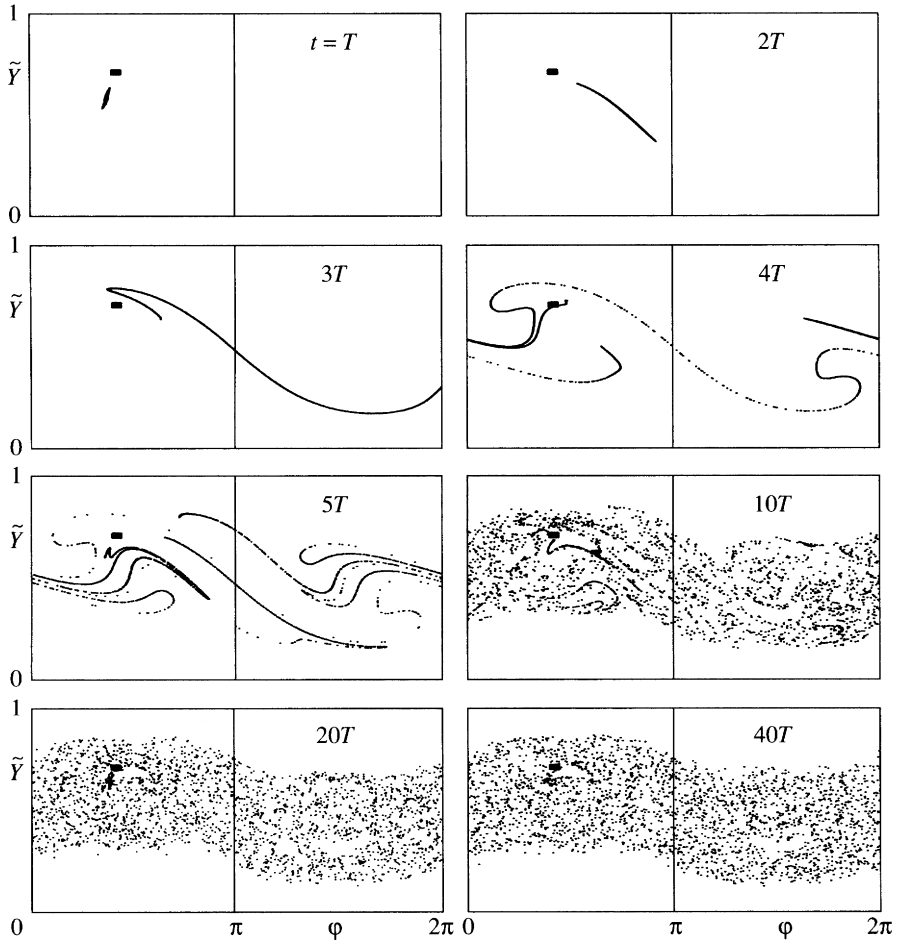

Fig. 6.

The numerical experiment agrees with these theoretical conclusions. In Fig. 2, M_3 and M_4 are actually hyperbolic-type points. For small ε chaos occurs in small neighbourhoods of these points. The regions of chaos increase as ε increases. When $\varepsilon \approx 0.5$ the area of chaos is a maximum. In this case all the fixed points M_1, M_2, M_3 and M_4 are unstable.

5. Mixing of the fluid particles

To describe the mixing we will solve the following problem. Consider a small rectangle of the phase plane with sides a and b: $\varphi_0 \le \varphi \le \varphi_0 + a$, $Y_0 \le Y \le Y_0 + b$. We will construct in this a grid, which divides each side into n equal sections. At the $n \times n$ nodes of the grid we place the initial Poincaré points and we photograph them over 1, 2, 3, $\cdots$, K periods. When there is no chaos these points will be situated in the neighbourhood of an invariant curve, passing through the chosen rectangle. An example of such a calculation for $\varepsilon = 0.1$ is shown in Fig. 5. The upper left corner of the initial rectangle is chosen to be at a point with coordinates $\varphi_0 = 0.2 \times 2\pi$, $Y_0 = 0.7$. The sides of the rectangle are one-fiftieth of the sides of the rectangular fluid-flow region, i.e. $a = 2\pi/50$ and $b = 1/50$. In a small rectangle, in the 50×50 nodes of the grid there are $51 \times 51 = 2601$ points. In the left upper corner of Fig. 5 there is a rectangle, filled with the initial points and points at which the fluid particles appear over a period. As can be seen, the rectangle with points has been converted in a period into an elongated parallelogram, i.e., over a period the rectangle, by a Poincaré mapping, becomes a parallelogram. Over two periods the region filled with points becomes an even more elongated parallelogram – a repeated Poincaré mapping of the parallelogram in the first period. This parallelogram is shown in the right upper corner of Fig. 5. In the following parts of Fig. 5 we show mappings of the initial points after 3, 4, 5, 10, 20 and 200 periods. It can be seen that the points are uniformly intermingled in a narrow curvilinear strip, the thickness of which is comparable with the dimensions of the small initial rectangle. The fluid particles can never penetrate outside this narrow strip. This regimé is not chaotic.

The next calculation for $\varepsilon = 0.5$ is shown in Fig. 6 and demonstrates good mixing of the fluid particles. The points of the rectangle located at this position after 10 periods are uniformly distributed over a wide area, comparable in area to the whole fluid-flow region. The mixing region corresponds to the phase portrait of the PPs when $\varepsilon = 0.5$ (see Fig. 2).

The results shown in Fig. 3 were obtained using a parametric mapping, which reduces the calculation time by a factor of approximately 100. For monitoring purposes we also carried out calculations using the Runge–Kutta scheme for the initial differential equations. The phase portraits obtained hardly differ.

6. Conclusion

The motion of particles of viscous fluid in a layer between eccentric rotating cylinders (Fig. 1) is described by the Hamilton Eq. (3.7). For a small eccentricity the Poincaré points are situated on invariant curves (Fig. 2) and there is no chaos. A Poincaré mapping over a period has four fixed points (Fig. 2): two of them elliptic

$$M_1(\varphi = \pi/2,\ Y = 1/2 + \varepsilon/4 + O(\varepsilon^3)), \quad M_2(\varphi = 3\pi/2,\ Y = 1/2 - \varepsilon/4 + O(\varepsilon^3))$$

and two of them hyperbolic

$$M_3(\varphi = 0,\ Y = 1/2 + O(\varepsilon^3)), \quad M_4(\varphi = \pi,\ Y = 1/2 + O(\varepsilon^3))$$

In the neighbourhood of hyperbolic points a beginning of a transition to dynamic chaos is observed when $\varepsilon > 0.2$. The area of the region of chaos of the Poincaré points increases as ε increases to a value of $\varepsilon \approx 0.5$.

A numerical calculation shows that when $\varepsilon = \varepsilon_0 \approx 0.5$ the points M_1 and M_2 become hyperbolic in a short interval $\Delta\varepsilon$. At this instant the area of chaos is a maximum. When $\varepsilon > \varepsilon_0 + \Delta\varepsilon$ the points M_1 and M_2 again become elliptic. The motion is ordered in the neighbourhood of these, and the area of chaos is correspondingly reduced.

Parametric Poincaré mappings enable one to calculate the fixed points, to investigate their stability and to describe the transition to chaos. The phase portraits of the Poincaré points, obtained using an analytical Poincaré mapping (Fig. 3), agree well with numerical experiments (Fig. 2).

The example considered is a mathematical model of a mixer for mixing media with high viscosity (more precisely, when conditions (1.4) are satisfied). The best mixing is obtained when $\varepsilon \approx 0.5$.

The parametric Poincaré mapping theory developed above enables the transition to dynamic chaos in similar types of hydrodynamic systems to be described.

Acknowledgements

I wish to thank D. M. Klimov and V. F. Zhuravlev for useful discussions.This research was financed by the Russian Foundation for Basic Reseach (08-01-00251).

References

1. Zhukovskii N Ye, *Complete Collected Papers. Vol. 3. Hydraulics*. Applied Mechanics. Moscow-Leningrad: Gostekhizdat; 1949.
2. Sommerfeld A. Zur hydrodynamischen Theorie der Schmiermittelreibung. *Z Math Phys* 1904;**50**(97):97–155.
3. Kochin NYe, Kibel IA, Roze NV. *Theoretical Hydromechanics Pt 2*. Moscow: Fizmatgiz; 1963.
4. Ballal BY, Rivlin RS. flow of a Newtonian fluid between eccentric rotating cylinders: Inertial effect. *Arch rat Mech Anal* 1976:237–94.
5. Loitsyanskii LG. *Mechanics of Liquids and Gases*. Oxford: Pergamon; 1978.
6. Kaper TJ, Wiggins S. An analytical study of transport in Stokes flows exhibiting large-scale chaos in the eccentric journal bearing. *J Fluid Mech* 1993;**253**:221–43.
7. Petrov AG. The Poincaré mapping method in hydrodynamic systems. Dynamic chaos in a fluid layer between eccentrically rotating cyinders. *Zh Prikl Mekh Fiz* 2003;**44**(1):3–21.
8. Klimov DM, Petrov AG, Georgiyevskii DV. *Viscoplastic Flows: Dynamic Chaos, Stability and Mixing*. Moscow: Nauka; 2005.

9. Landau LD, Lifshitz EM. *Fluid Dynamics*. Oxford: Perganmon; 1987.
10. Zaslavskii GM. *Stochastic Bahavior of Dynamical Systems*. New York: Harwood; 1983.
11. Ottino JM. *The Kinematics of Mixing: Stretching, Chaos and Transport*. Cambridge: Univ. Press; 1989, 359.
12. Lichtenberg AJ, Lieberman MA. *Regular and Chaotic Motion*. New York: Springer; 1983.
13. Shuster HJ. *Deterministic Chaos: An Introduction*. Weinheiheim: Physik-Verlag; 1984.
14. Petrov AG. The parametric method of Poincaré mappings in hydrodynamic systems. *Prikl Mat Mekh* 2002;**66**(6):356–65.

Translated by R.C.G.